J Mater Sci (2008) 43:7286–7292
DOI 10.1007/s10853-008-2624-z

ULTRAFINE-GRAINED MATERIALS

Evaluating the influence of pressure and torsional strain on processing by high-pressure torsion

Cheng Xu · Zenji Horita · Terence G. Langdon

Received: 28 February 2008 / Accepted: 28 March 2008 / Published online: 13 July 2008

Abstract Tests were conducted on an Al-6061 alloy to evaluate the separate effects of the applied pressure and the torsional straining in processing by high-pressure torsion (HPT). The values of the Vickers microhardness were measured after processing and plotted both linearly across the diameters of the disks and as three-dimensional representations. The measurements show that the applied pressure increases the hardness in the absence of torsional straining. In the presence of a pressure and torsional straining, the hardness values are high at the edges of the disk but lower in the central region. There is a gradual evolution toward a hardness homogeneity with increasing numbers of HPT revolutions. The hardness values at the edges of the disks are reasonably independent of the applied pressure but the extent of this region of high hardness depends upon both the applied pressure and the numbers of turns in the HPT processing.

Introduction

Very significant grain refinement may be achieved by processing bulk metals through the application of severe plastic deformation (SPD) [1]. Typically, the grains achieved in SPD processing are in the submicrometer or even the nanometer range. Several SPD processes are now available but the most common procedure in current use is equal-channel angular pressing (ECAP) [2]. However, there is very good evidence showing that the alternative process of high-pressure torsion [3] is especially attractive because it leads to even finer grain sizes than those achieved in ECAP. For example, there are reports of the occurrence of grain sizes of $\sim$300 nm in ECAP and $\sim$100 nm in HPT in an Al-5% Fe alloy [4] and $\sim$350 nm in ECAP and $\sim$170 nm in HPT in high-purity Ni [5].

Processing by HPT is rapidly becoming an attractive procedure for the fabrication of fully-dense materials having exceptionally small grain sizes. However, the fundamental properties of HPT are not yet fully documented. Accordingly, the present investigation was undertaken to evaluate the separate influences of pressure and torsional strain in HPT processing.

Principles of processing by HPT

The principle of HPT processing is illustrated schematically by the cross-sectional view as shown in Fig. 1. Two large anvils are constructed with the inner surfaces nitrided to provide surface hardening and excellent dimensional control. The sample, in the form of a thin disk, is then placed in a depression in the lower anvil and this anvil is brought upwards so that the sample is encased in an equal depression on the lower face of the upper anvil. When in position as shown in Fig. 1, there is a small gap between the faces of the upper and lower anvils so that on application of a high pressure, P, there is a minor outflow of material around the periphery of the disk. Torsional

C. Xu (✉) · T. G. Langdon
Departments of Aerospace and Mechanical Engineering and Materials Science, University of Southern California, Los Angeles, CA 90089-1453, USA
e-mail: chengxu@usc.edu

Z. Horita
Department of Materials Science and Engineering, Faculty of Engineering, Kyushu University, Fukuoka 819-0395, Japan

T. G. Langdon
Materials Research Group, School of Engineering Sciences, University of Southampton, Southampton SO17 1BJ, UK

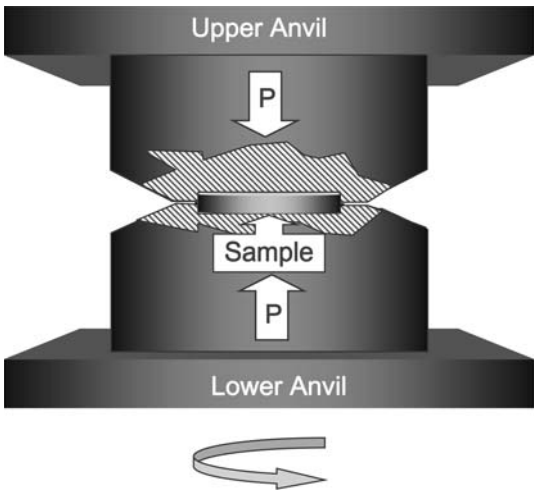

Fig. 1 Schematic illustration of the HPT facility

straining is then undertaken by rotation of the lower anvil. The illustration depicted in Fig. 1 represents constrained HPT in which the sample is held in place by the anvils and straining effectively takes place under the presence of a back-pressure [6]. Due to the limited outward flow of material occurring at the edge of the disk, this situation is more accurately described as quasi-constrained HPT. It is apparent from Fig. 1 that processing by HPT therefore combines two critical and inter-related steps: first there is an application of the pressure P and second, and concurrently, there is a torsional straining.

An important critical question in HPT concerns the ability to attain a homogeneous microstructure throughout the disk after processing. In principle, it is reasonable to anticipate it may be impossible to achieve homogeneity in HPT disks. This is because the equivalent von Mises strain, ε_{eq}, imposed on the disk through torsional straining is given by the relationship [7, 8]

$$\varepsilon_{eq} = \frac{2\pi Nr}{h\sqrt{3}}, \quad (1)$$

where r is the radius of the disk, h the height of the disk, and N is the number of turns imposed in torsional straining.

It follows from Eq. 1 that the strain varies with radius and at the center of the disk, where $r = 0$, the strain is zero. Nevertheless, despite this very marked variation in the imposed torsional strain, there is experimental evidence suggesting that, after the application of a sufficient number of turns, the microstructure may evolve and attain a reasonable level of homogeneity. There are now several reports documenting an evolution to homogeneity across the total area of the disk in processing by HPT [3, 6, 9–12] although other reports describe very significant inhomogeneities [13–15].

It is apparent from the preceding description that two distinct and critical steps are involved in processing by HPT due to the application of the imposed pressure and the subsequent torsional straining. Although both of these parameters are important, there have been no systematic tests to isolate the influence of these two steps by evaluating the effect of the imposed pressure in the absence of any torsional straining. The present investigation was undertaken to provide this information by examining the evolution of homogeneity in an aluminum alloy under a range of different processing conditions.

An earlier report on homogeneity in samples processed by ECAP demonstrated a good correlation between hardness measurements taken on polished surfaces of the ECAP samples and microstructural observations undertaken using transmission electron microscopy (TEM) [16]. As a consequence of this correlation, and as in an earlier study after processing by ECAP [17], it is reasonable to consider that the development of a hardness homogeneity in the sample corresponds also to the development of an essentially homogeneous microstructure.

Experimental material and procedures

The experiments were conducted using a commercial aluminum 6061 alloy containing, in wt.%, 1.01% Mg, 0.59% Si, 0.37% Fe, 0.29% Cu, 0.23% Cr, and 0.20% Zn: further details about this material were given in an earlier report [16]. Prior to processing by HPT, the material was annealed at 693 K for 4 h with a heating and cooling rate of 10 K h^{-1} to give an initial grain size of $\sim$50 μm. Disks were prepared for HPT having diameters of 10 mm and thicknesses of $\sim$0.90 mm. The processing by HPT was conducted at room temperature under pressures up to a maximum of 4.0 GPa using the facility described earlier where torsional straining is applied using a rotation speed of 1 rpm [10].

Two different types of tests were conducted. First, to isolate the effect of the imposed pressure, tests were performed by applying a selected pressure for a period of 1 min without torsional straining where this period was chosen because it is equivalent to the time required for one revolution in HPT. Second, to evaluate the evolution of homogeneity under HPT processing, disks were subjected to imposed pressures of either 1.25 or 4.0 GPa and they were then strained in torsion by rotation of the lower anvil through either one or five turns. Careful measurements showed the thicknesses of the disks were $\sim$0.89 mm after testing through any of these various procedures.

Following HPT, the disks were mounted and carefully polished to a mirror-like finish. Microhardness measurements were taken using an FM-1e microhardness tester equipped with a Vickers indenter. Two different sets of measurements were recorded. First, a series of individual

measurements was recorded on each polished surface in which measurements of the Vickers microhardness, Hv, were recorded across the diameter of each disk using incremental steps between the measurements of 0.3 mm. For these measurements, Hv was recorded at four locations uniformly positioned around each selected point and at distances of 0.15 mm from the chosen point. These four measurements were then averaged and the error bars were calculated as the 95% confidence limits. Second, measurements of Hv were recorded at distances of 0.30 mm along two sets of parallel lines forming a regular rectilinear grid pattern defined by the coordinate axes X and Y, where these two axes were established parallel to two perpendicular diameters on the surface of each disk with the position (0, 0) corresponding to the center of each sample. For this procedure, a single measurement of Hv was recorded at each point with the points separated by a spacing of 0.30 mm in two mutually perpendicular directions.

For the measurements taken along linear traverses, the data points and the associated error bars were plotted as the hardness value against the distance from the center of the disk. For the measurements taken following a rectilinear grid pattern, the data were plotted as Hv against the individual values of X and Y in a three-dimensional format.

Experimental results

Using the data recorded over the whole surfaces of the disks, Table 1 shows the average values of the microhardness for the various testing conditions used in this investigation, where the bottom line denotes the unprocessed and annealed condition and the line for $N = 0$ represents the values of Hv after applying pressures of either 1.25 or 4.0 GPa without any torsional straining.

Several conclusions may be drawn from the results in Table 1. First, the average hardness increases significantly on imposition of an applied pressure even in the absence of any torsional straining. Specifically, the values of Hv increase by $\sim$55% and $\sim$80% on application of pressures of 1.25 and 4.0 GPa, respectively. Second, the error bars are significantly larger after applying a pressure without torsional straining by comparison with the error bar in the unprocessed material. This demonstrates the development of some local inhomogeneities during the pressing operation. Third, in the absence of torsional straining where $N = 0$ there are larger error bars on the disk subjected to the higher pressure. This is undoubtedly associated with the use of a quasi-constrained HPT facility which permits a small outflow of material on application of the pressure. Fourth, there is a further very significant increase in hardness on applying torsional straining through one turn and again an additional increase when the straining is applied through a total of five turns. It is important to note that the final values of Hv are very similar for both imposed pressures after five turns of torsional straining and these values, where the Vickers microhardness is Hv $\approx$ 165–170, represent an increase by a factor of $\sim$2.7$\times$ by comparison with the initial material.

Table 1 The average microhardness values for Al-6061 before and after HPT

Number of turns (N)	Vickers microhardness (Hv)	
	P = 1.25 GPa	P = 4.0 GPa
0	70.1 ± 1.5	81.2 ± 1.9
1	146.4 ± 3.6	127.4 ± 3.9
5	165.1 ± 2.0	170.3 ± 1.5
Unprocessed	44.7 ± 0.2	

A more complete description of these hardness data may be achieved by plotting the individual hardness values and their error bars against the location along linear traverses across the disks as shown in Fig. 2a and b for pressures of 1.25 and 4.0 GPa, respectively. In these plots, the lower solid points denote the unprocessed and annealed condition, the points labeled $N = 0$ correspond to the application of a pressure for 1 min in the absence of torsional straining and the remaining data denote linear traverses after one and five turns, respectively.

It is immediately apparent from Fig. 2 that the unprocessed material exhibits excellent homogeneity. For the samples processed under high pressures without any torsional straining where $N = 0$, there are reasonable levels of homogeneity in the hardness distributions across the disks although in both conditions there is a tendency to record slightly higher values of Hv at the edges of the disks. This increase in hardness around the periphery is a direct consequence of the outflow of material and the consequent higher level of deformation within this region. In contrast, the upper plots for the samples subjected to torsional straining show significant variations in the hardness distributions across the disks.

In general, it appears that the hardness distributions may be divided into three reasonably distinct regions based on concentric circles around the mid-point of each disk: there is a central region where the values of Hv are low although slightly higher than after imposition of the pressure without torsional straining, there is an intermediate region where the hardness values increase and there is an outer peripheral region near the edges of the disks where there is a very high value of Hv. It is significant to note that the values of Hv at the outer edges and in the central region are essentially the same after either one or five turns and after imposed pressures of either 1.25 or 4.0 GPa. In contrast, in

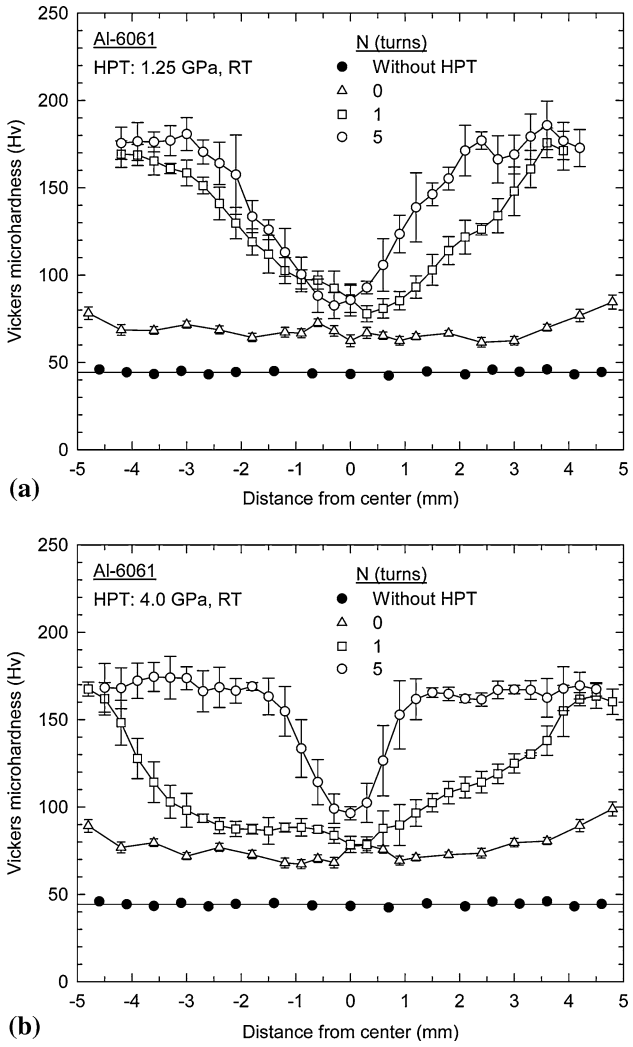

Fig. 2 The average Vickers microhardness, Hv, versus distance from the center of the Al-6061 disk in the unprocessed condition, after applying a pressure without torsional straining and after applying a pressure and concurrent torsional straining for up to five turns at pressures of (**a**) 1.25 and (**b**) 4.0 GPa

the intermediate transition regions there are very marked differences depending upon the precise testing conditions. Thus, the width of the edge region having higher hardness tends to extend inwards and become broader with increasing numbers of turns and this is especially apparent at the higher pressure of 4.0 GPa as shown in Fig. 2b where the edge region extends inwards through ~3.5 mm when straining through a total of five turns. In contrast, there is only a small increase with increasing numbers of turns in the values of the lowest hardness recorded in the centers of the disks when increasing the straining from one to five turns. Moreover, it is apparent that the error bars for the edge region remain relatively unchanged under different processing conditions, while the error bars for the intermediate transition region tend to increase with increasing numbers of turns for the two different applied pressures.

It is convenient to take the results for the microhardness measurements over the entire surfaces of the samples and present these data in a three-dimensional representation whereby the individual values of Hv are plotted against the position of each point defined in terms of the X and Y coordinate axes. An example of this procedure is shown in Fig. 3a and b for the disks subjected to a pressure for 1 min without torsional straining at 1.25 and 4.0 GPa, respectively. Similar plots are given in Fig. 4 for a pressure of 1.25 GPa after (a) one and (b) five turns and for a pressure of 4.0 GPa after (c) one and (d) five turns, respectively.

It is apparent from Fig. 3 that the samples exhibit homogenous hardness distributions over major fractions of the disks after applying a high pressure without torsional straining but in Fig. 4 there are clearly very significant differences in the hardness distributions for the various processing conditions. Specifically, these three-dimensional displays demonstrate the evolution with additional straining toward a more homogeneous structure and, in addition, they show that the central region of lower hardness becomes smaller in area when the total applied pressure is increased. Thus, at a pressure of $P = 4.0$ GPa for $N = 5$ turns the central region of lower hardness has a diameter of only ~1 mm as shown in Fig. 4d.

Discussion

The compressive strain introduced into the HPT disk during application of the external pressure reduced the disk thickness from, typically, ~0.90 to ~0.89 mm corresponding to a reduction in height of ~1.1%. This strain is exceptionally small by comparison with the very large shear strains subsequently introduced during the HPT processing. Nevertheless, this relatively small compressive strain led to an overall increase in the hardness of the disk by ~55–80% depending upon the precise level of the applied stress. Although this increase in hardness is small by comparison with the much larger increase, by a factor of >2×, introduced by torsional straining, it is by no means a negligible contribution and it should be included in any detailed analysis. Furthermore, it is apparent from the results in Table 1 that the increase in hardness due to the applied pressure increases significantly at the higher pressure of 4.0 GPa whereas, in contrast, the final hardness values at the peripheries of the disks appear to be almost independent of the applied pressure at least within the pressure range from 1.25 to 4.0 GPa.

These measurements show, therefore, that the external applied pressure has a relatively minor influence on the values of the final equilibrium hardness at the edges of the

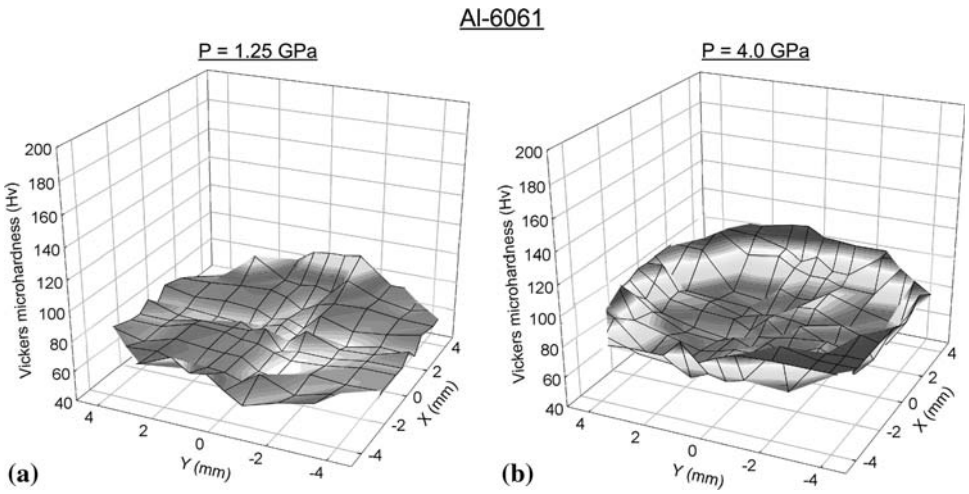

Fig. 3 Three-dimensional representations of the hardness distributions across the Al-6061 disks after processing for 1 min without torsional straining at pressures of (**a**) 1.25 and (**b**) 4.0 GPa

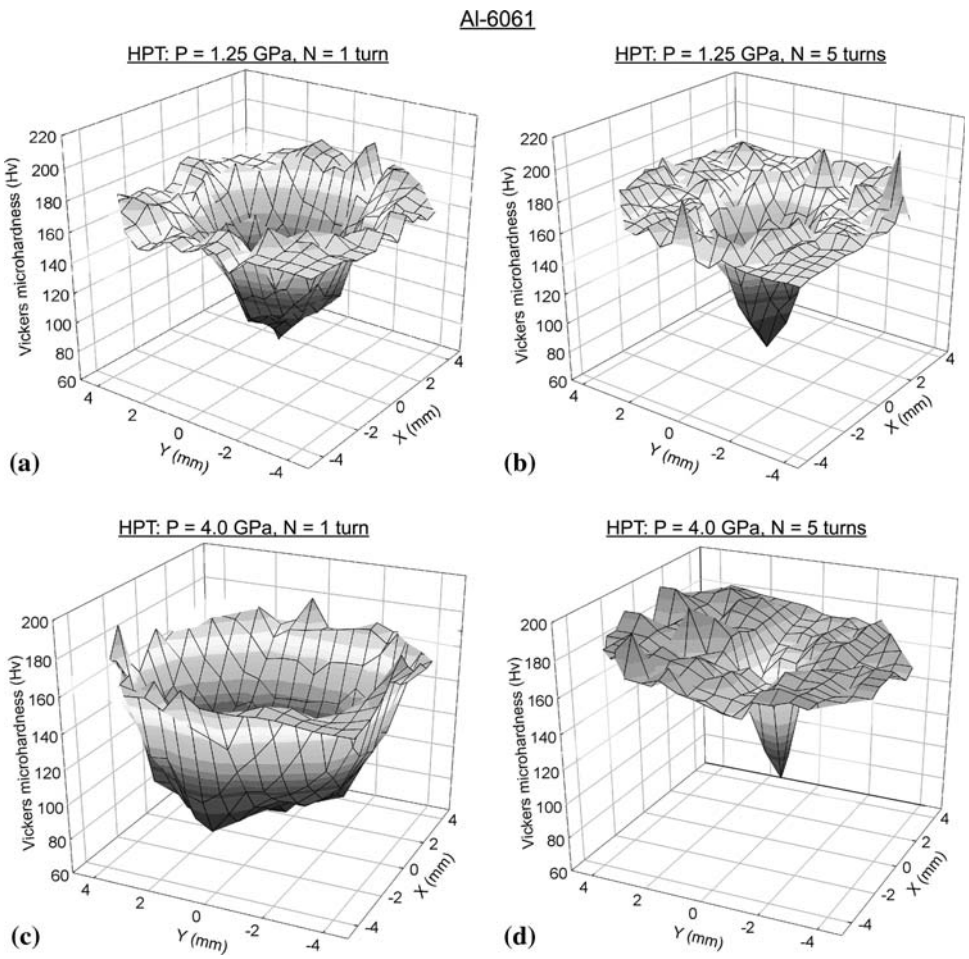

Fig. 4 Three-dimensional representations of the hardness distributions across the Al-6061 disks after applying a pressure of 1.25 GPa for totals of (**a**) one and (**b**) five turns and applying a pressure of 4.0 GPa for totals of (**c**) one and (**d**) five turns

disks but it is apparent from Fig. 2 that the pressure is critical in determining the rate at which the hardness values in the center of the disk increase toward this equilibrium value.

An important conclusion from these results is that the values of the Vickers microhardness are lower in the center of the disk by comparison with the outer region. This result is contrary to the data reported earlier for high purity Al [12] where the hardness was higher in the center of the disk but it is consistent with the results reported for several other materials exhibiting lower values of hardness in the disk centers including commercial purity aluminum and aluminum-based alloys [6, 10, 11, 18, 19], copper and copper-based alloys [13, 20–23], pure Ni [3, 9, 15],

austenitic steel [14], low-carbon steel [24], Ti [24], and a Ti-based nanocomposite [25]. There are some recent results demonstrating lower hardness values at the peripheries of HPT disks for a Cu–Zr–Ti alloy but these results are not generally representative because they arise from a local amorphization within this outer region [26].

It was shown earlier that the higher hardness values observed in the disk centers for high-purity aluminum are consistent with the smaller grains observed in this region by TEM [12] and it was proposed that the different results recorded for high-purity aluminum reflect the very high stacking fault energy and hence the rapid dynamic recovery occurring within the ultrafine-grained substructure introduced around the disk periphery. This conclusion was also consistent with the TEM observations of high-purity Al because the central region of the disk showed lattice distortions and a high density of intragranular dislocations whereas the grains around the edge were almost free of dislocations and the microstructure appeared to be in a low-energy configuration. The present results on the Al-6061 alloy are consistent with this earlier interpretation.

An important question in HPT processing concerns the ability to attain macroscopic homogeneity throughout the HPT disk. Based on measurements of the Vickers microhardness, excellent homogeneity was achieved in the earlier experiments on high-purity Al after processing through five turns at a pressure of 1.25 GPa [12], but in the present investigation this same testing condition resulted in a small central region of lower hardness as shown in Fig. 4b. The extent of this region of lower hardness covered a central diameter of $\sim$1 mm in the present tests on the Al-6061 alloy. It is reasonable to conclude from Figs. 2 and 4 that it is probably feasible to achieve an overall homogeneity throughout the disks of the Al-6061 alloy if the torsional straining is continued to a sufficiently large number of turns. Furthermore, this gradual transition toward homogeneity is consistent with the reported change in the nature of the tensile stress–strain curves for samples of pure titanium strained through different numbers of HPT revolutions [27].

Summary and conclusions

1. Samples of an Al-6061 alloy were processed under two different conditions: (i) under different applied pressures but without torsional straining for 1 min and (ii) with an applied pressure and concurrent torsional straining for up to five turns. The values of the Vickers microhardness, Hv, were plotted both linearly across the diameters of the disks and using a three-dimensional representation for different conditions of imposed pressure and numbers of turns.
2. The results reveal an increase in hardness and a reasonably homogeneous hardness distribution for disks subjected only to an applied external pressure. After applying a pressure and concurrent torsional straining, the hardness values are high around the disk periphery but lower values are recorded in the central regions.
3. There is an evolution toward a hardness homogeneity with increasing numbers of turns in HPT processing. The hardness values recorded at the outer edges of the disks are reasonably independent of the magnitude of the applied pressure, but the extent of this region of high hardness depends critically upon both the applied pressure and the number of revolutions.

Acknowledgements This work was supported in part by the Light Metals Educational Foundation of Japan, in part by a Grant-in-Aid for Scientific Research from the Ministry of Education, Culture, Sports, Science and Technology, Japan, in the Priority Area "Giant Straining Process for Advanced Materials Containing Ultra-High Density Lattice Defects" and in part by the National Science Foundation of the United States under Grant no. DMR-0243331.

References

1. Valiev RZ, Islamgaliev RK, Alexandrov IV (2000) Prog Mater Sci 45:103. doi:10.1016/S0079-6425(99)00007-9
2. Valiev RZ, Langdon TG (2006) Prog Mater Sci 51:881. doi:10.1016/j.pmatsci.2006.02.003
3. Zhilyaev AP, Nurislamova GV, Kim BK, Baró MD, Szpunar JA, Langdon TG (2003) Acta Mater 51:753. doi:10.1016/S1359-6454(02)00466-4
4. Stolyarov VV, Valiev RZ (2004) In: Zehetbauer MJ, Valiev RZ (eds) Nanomaterials by severe plastic deformation. Willey-VCH, Weinheim, p 125
5. Zhilyaev AP, Kim BK, Nurislamova GV, Baró MD, Szpunar JA, Langdon TG (2002) Scripta Mater 48:575
6. Zhilyaev AP, Oh-Ishi K, Langdon TG, McNelley TR (2005) Mater Sci Eng A410–A411:277. doi:10.1016/j.msea.2005.08.044
7. Valiev RZ, Ivanisenko YuV, Rauch EF, Baudelet B (1996) Acta Mater 44:4705. doi:10.1016/S1359-6454(96)00156-5
8. Wetscher F, Vorhauer A, Stock R, Pippan A (2004) Mater Sci Eng A387–A389:809. doi:10.1016/j.msea.2004.01.096
9. Zhilyaev AP, Lee S, Nurislamova GV, Valiev RZ, Langdon TG (2001) Scripta Mater 44:2753. doi:10.1016/S1359-6462(01)00955-1
10. Sakai G, Horita Z, Langdon TG (2005) Mater Sci Eng A393:344. doi:10.1016/j.msea.2004.11.007
11. Horita Z, Langdon TG (2005) Mater Sci Eng A410–A411:422. doi:10.1016/j.msea.2005.08.133
12. Xu C, Horita Z, Langdon TG (2007) Acta Mater 55:203. doi:10.1016/j.actamat.2006.07.029
13. Jiang H, Zhu YT, Butt DP, Alexandrov IV, Lowe TC (2000) Mater Sci Eng A290:128. doi:10.1016/S0921-5093(00)00919-9
14. Vorhauer A, Pippan R (2004) Scripta Mater 51:921. doi:10.1016/j.scriptamat.2004.04.025
15. Yang Z, Welzel U (2005) Mater Lett 59:3406. doi:10.1016/j.matlet.2005.05.077
16. Xu C, Furukawa M, Horita Z, Langdon TG (2005) Mater Sci Eng A398:66. doi:10.1016/j.msea.2005.03.083

17. Xu C, Langdon TG (2007) J Mater Sci 42:1542. doi:10.1007/s10853-006-0899-5
18. Zhilyaev AP, McNelley TR, Langdon TG (2007) J Mater Sci 42:1517. doi:10.1007/s10853-006-0628-0
19. Todaka Y, Umemoto M, Yamazaki A, Sasaki J, Tsuchiya K (2008) Mater Trans 49:7. doi:10.2320/matertrans.ME200713
20. Čížek J, Procházka I, Brauer G, Anwand W, Kužel R, Cieslar M, Islamgaliev RK (2003) Phys Stat Sol A 195:335. doi:10.1002/pssa.200305929
21. Degtyarev MV, Chashchukhina TI, Voronova LM, Patselov AM, Pilyugin VP (2007) Acta Mater 55:6039. doi:10.1016/j.actamat.2007.04.017
22. Ungár T, Balogh L, Zhu YT, Horita Z, Xu C, Langdon TG (2007) Mater Sci Eng A444:153. doi:10.1016/j.msea.2006.08.059
23. Balogh L, Ungár T, Zhao Y, Zhu YT, Horita Z, Xu C, Langdon TG (2008) Acta Mater 56:809
24. Todaka Y, Umemoto M, Yamazaki A, Sasaki J, Tsuchiya K (2008) Mater Trans 49:47. doi:10.2320/matertrans.ME200714
25. Concustell A, Sort J, Suriñach S, Gebert A, Eckert J, Zhilyaev AP, Baró MD (2007) Intermetallics 15:1038. doi:10.1016/j.intermet.2006.12.009
26. Kovács Zs, Hóbor S, Szabó PJ, Lendvai J, Zhilyaev AP, Révész Á (2007) Mater Sci Eng A449–A451:1139. doi:10.1016/j.msea.2006.03.133
27. Valiev RZ, Alexandrov IV, Zhu YT, Lowe TC (2002) J Mater Res 17:5